Measurements of ψ^{′}→p[over ¯]K^{+}Σ^{0} and χ_{cJ}→p[over ¯]K^{+}Λ

M. Ablikim *et al.* (BESIII Collaboration)

Phys. Rev. D **87**, 012007 — Published 18 January 2013

DOI: 10.1103/PhysRevD.87.012007

Measurements of $\psi' \to \bar{p}K^+\Sigma^0$ and $\chi_{cJ} \to \bar{p}K^+\Lambda$

M. Ablikim[1], M. N. Achasov[6], O. Albayrak[3], D. J. Ambrose[39], F. F. An[1], Q. An[40], J. Z. Bai[1], Y. Ban[26], J. Becker[2], J. V. Bennett[16], M. Bertani[17A], J. M. Bian[38], E. Boger[19,a], O. Bondarenko[20], I. Boyko[19], R. A. Briere[3], V. Bytev[19], X. Cai[1], O. Cakir[34A], A. Calcaterra[17A], G. F. Cao[1], S. A. Cetin[34B], J. F. Chang[1], G. Chelkov[19,a], G. Chen[1], H. S. Chen[1], J. C. Chen[1], M. L. Chen[1], S. J. Chen[24], X. Chen[26], Y. B. Chen[1], H. P. Cheng[14], Y. P. Chu[1], D. Cronin-Hennessy[38], H. L. Dai[1], J. P. Dai[1], D. Dedovich[19], Z. Y. Deng[1], A. Denig[18], I. Denysenko[19,b], M. Destefanis[43A,43C], W. M. Ding[28], Y. Ding[22], L. Y. Dong[1], M. Y. Dong[1], S. X. Du[46], J. Fang[1], S. S. Fang[1], L. Fava[43B,43C], C. Q. Feng[40], R. B. Ferroli[17A], P. Friedel[2], C. D. Fu[1], Y. Gao[33], C. Geng[40], K. Goetzen[7], W. X. Gong[1], W. Gradl[18], M. Greco[43A,43C], M. H. Gu[1], Y. T. Gu[9], Y. H. Guan[36], A. Q. Guo[25], L. B. Guo[23], T. Guo[23], Y. P. Guo[25], Y. L. Han[1], F. A. Harris[37], K. L. He[1], M. He[1], Z. Y. He[25], T. Held[2], Y. K. Heng[1], Z. L. Hou[1], C. Hu[23], H. M. Hu[1], J. F. Hu[35], T. Hu[1], G. M. Huang[4], G. S. Huang[40], J. S. Huang[12], L. Huang[1], X. T. Huang[28], Y. Huang[24], Y. P. Huang[1], T. Hussain[42], C. S. Ji[40], Q. Ji[1], Q. P. Ji[25], X. B. Ji[1], X. L. Ji[1], L. L. Jiang[1], X. S. Jiang[1], J. B. Jiao[28], Z. Jiao[14], D. P. Jin[1], S. Jin[1], F. F. Jing[33], N. Kalantar-Nayestanaki[20], M. Kavatsyuk[20], B. Kopf[2], M. Kornicer[37], W. Kuehn[35], W. Lai[1], J. S. Lange[35], M. Leyhe[2], C. H. Li[1], Cheng Li[40], Cui Li[40], D. M. Li[46], F. Li[1], G. Li[1], H. B. Li[1], J. C. Li[1], K. Li[10], Lei Li[1], Q. J. Li[1], S. L. Li[1], W. D. Li[1], W. G. Li[1], X. L. Li[28], X. N. Li[1], X. Q. Li[25], X. R. Li[27], Z. B. Li[32], H. Liang[40], Y. F. Liang[30], Y. T. Liang[35], G. R. Liao[33], X. T. Liao[1], D. Lin[11], B. J. Liu[1], C. L. Liu[3], C. X. Liu[1], F. H. Liu[29], Fang Liu[1], Feng Liu[4], H. Liu[1], H. B. Liu[9], H. H. Liu[13], H. M. Liu[1], H. W. Liu[1], J. P. Liu[44], K. Liu[33], K. Y. Liu[22], Kai Liu[36], P. L. Liu[28], Q. Liu[36], S. B. Liu[40], X. Liu[21], Y. B. Liu[25], Z. A. Liu[1], Zhiqiang Liu[1], Zhiqing Liu[1], H. Loehner[20], G. R. Lu[12], H. J. Lu[14], J. G. Lu[1], Q. W. Lu[29], X. R. Lu[36], Y. P. Lu[1], C. L. Luo[23], M. X. Luo[45], T. Luo[37], X. L. Luo[1], M. Lv[1], C. L. Ma[36], F. C. Ma[22], H. L. Ma[1], Q. M. Ma[1], S. Ma[1], T. Ma[1], X. Y. Ma[1], F. E. Maas[11], M. Maggiora[43A,43C], Q. A. Malik[42], Y. J. Mao[26], Z. P. Mao[1], J. G. Messchendorp[20], J. Min[1], T. J. Min[1], R. E. Mitchell[16], X. H. Mo[1], C. Morales Morales[11], K. Moriya[16], N. Yu. Muchnoi[6], H. Muramatsu[39], Y. Nefedov[19], C. Nicholson[36], I. B. Nikolaev[6], Z. Ning[1], S. L. Olsen[27], Q. Ouyang[1], S. Pacetti[17B], J. W. Park[27], M. Pelizaeus[2], H. P. Peng[40], K. Peters[7], J. L. Ping[23], R. G. Ping[1], R. Poling[38], E. Prencipe[18], M. Qi[24], S. Qian[1], C. F. Qiao[36], L. Q. Qin[28], X. S. Qin[1], Y. Qin[26], Z. H. Qin[1], J. F. Qiu[1], K. H. Rashid[42], G. Rong[1], X. D. Ruan[9], A. Sarantsev[19,c], B. D. Schaefer[16], M. Shao[40], C. P. Shen[37,d], X. Y. Shen[1], H. Y. Sheng[1], M. R. Shepherd[16], X. Y. Song[1], S. Spataro[43A,43C], B. Spruck[35], D. H. Sun[1], G. X. Sun[1], J. F. Sun[12], S. S. Sun[1], Y. J. Sun[40], Y. Z. Sun[1], Z. J. Sun[1], Z. T. Sun[40], C. J. Tang[30], X. Tang[1], I. Tapan[34C], E. H. Thorndike[39], D. Toth[38], M. Ullrich[35], G. S. Varner[37], B. Q. Wang[26], D. Wang[26], D. Y. Wang[26], K. Wang[1], L. L. Wang[1], L. S. Wang[1], M. Wang[28], P. Wang[1], P. L. Wang[1], Q. J. Wang[1], S. G. Wang[26], X. F. Wang[33], X. L. Wang[40], Y. F. Wang[1], Z. Wang[1], Z. G. Wang[1], Z. Y. Wang[1], D. H. Wei[8], J. B. Wei[26], P. Weidenkaff[18], Q. G. Wen[40], S. P. Wen[1], M. Werner[35], U. Wiedner[2], L. H. Wu[1], N. Wu[1], S. X. Wu[40], W. Wu[25], Z. Wu[1], L. G. Xia[33], Y. X Xia[15], Z. J. Xiao[23], Y. G. Xie[1], Q. L. Xiu[1], G. F. Xu[1], G. M. Xu[26], Q. J. Xu[10], Q. N. Xu[36], X. P. Xu[31], Z. R. Xu[40], F. Xue[4], Z. Xue[1], L. Yan[40], W. B. Yan[40], Y. H. Yan[15], H. X. Yang[1], Y. Yang[4], Y. X. Yang[8], H. Ye[1], M. Ye[1], M. H. Ye[5], B. X. Yu[1], C. X. Yu[25], H. W. Yu[26], J. S. Yu[21], S. P. Yu[28], C. Z. Yuan[1], Y. Yuan[1], A. A. Zafar[42], A. Zallo[17A], Y. Zeng[15], B. X. Zhang[1], B. Y. Zhang[1], C. Zhang[24], C. C. Zhang[1], D. H. Zhang[1], H. H. Zhang[32], H. Y. Zhang[1], J. Q. Zhang[1], J. W. Zhang[1], J. Y. Zhang[1], J. Z. Zhang[1], LiLi Zhang[15], R. Zhang[36], S. H. Zhang[1], X. J. Zhang[1], X. Y. Zhang[28], Y. Zhang[1], Y. H. Zhang[1], Z. P. Zhang[40], Z. Y. Zhang[44], Zhenghao Zhang[4], G. Zhao[1], H. S. Zhao[1], J. W. Zhao[1], K. X. Zhao[23], Lei Zhao[40], Ling Zhao[1], M. G. Zhao[25], Q. Zhao[1], Q. Z. Zhao[9], S. J. Zhao[46], T. C. Zhao[1], Y. B. Zhao[1], Z. G. Zhao[40], A. Zhemchugov[19,a], B. Zheng[41], J. P. Zheng[1], Y. H. Zheng[36], B. Zhong[23], Z. Zhong[9], L. Zhou[1], X. K. Zhou[36], X. R. Zhou[40], C. Zhu[1], K. Zhu[1], K. J. Zhu[1], S. H. Zhu[1], X. L. Zhu[33], Y. C. Zhu[40], Y. M. Zhu[25], Y. S. Zhu[1], Z. A. Zhu[1], J. Zhuang[1], B. S. Zou[1], J. H. Zou[1]

(BESIII Collaboration)

[1] *Institute of High Energy Physics, Beijing 100049, People's Republic of China*
[2] *Bochum Ruhr-University, D-44780 Bochum, Germany*
[3] *Carnegie Mellon University, Pittsburgh, Pennsylvania 15213, USA*
[4] *Central China Normal University, Wuhan 430079, People's Republic of China*
[5] *China Center of Advanced Science and Technology, Beijing 100190, People's Republic of China*
[6] *G.I. Budker Institute of Nuclear Physics SB RAS (BINP), Novosibirsk 630090, Russia*
[7] *GSI Helmholtzcentre for Heavy Ion Research GmbH, D-64291 Darmstadt, Germany*
[8] *Guangxi Normal University, Guilin 541004, People's Republic of China*
[9] *GuangXi University, Nanning 530004, People's Republic of China*
[10] *Hangzhou Normal University, Hangzhou 310036, People's Republic of China*
[11] *Helmholtz Institute Mainz, Johann-Joachim-Becher-Weg 45, D-55099 Mainz, Germany*
[12] *Henan Normal University, Xinxiang 453007, People's Republic of China*
[13] *Henan University of Science and Technology, Luoyang 471003, People's Republic of China*
[14] *Huangshan College, Huangshan 245000, People's Republic of China*
[15] *Hunan University, Changsha 410082, People's Republic of China*
[16] *Indiana University, Bloomington, Indiana 47405, USA*
[17] *(A)INFN Laboratori Nazionali di Frascati, I-00044, Frascati, Italy; (B)INFN and University of Perugia, I-06100, Perugia, Italy*
[18] *Johannes Gutenberg University of Mainz, Johann-Joachim-Becher-Weg 45, D-55099 Mainz, Germany*
[19] *Joint Institute for Nuclear Research, 141980 Dubna, Moscow region, Russia*
[20] *KVI, University of Groningen, NL-9747 AA Groningen, The Netherlands*

[21] Lanzhou University, Lanzhou 730000, People's Republic of China
[22] Liaoning University, Shenyang 110036, People's Republic of China
[23] Nanjing Normal University, Nanjing 210023, People's Republic of China
[24] Nanjing University, Nanjing 210093, People's Republic of China
[25] Nankai University, Tianjin 300071, People's Republic of China
[26] Peking University, Beijing 100871, People's Republic of China
[27] Seoul National University, Seoul, 151-747 Korea
[28] Shandong University, Jinan 250100, People's Republic of China
[29] Shanxi University, Taiyuan 030006, People's Republic of China
[30] Sichuan University, Chengdu 610064, People's Republic of China
[31] Soochow University, Suzhou 215006, People's Republic of China
[32] Sun Yat-Sen University, Guangzhou 510275, People's Republic of China
[33] Tsinghua University, Beijing 100084, People's Republic of China
[34] (A)Ankara University, Dogol Caddesi, 06100 Tandogan, Ankara, Turkey; (B)Dogus University, 34722 Istanbul, Turkey; (C)Uludag University, 16059 Bursa, Turkey
[35] Universitaet Giessen, D-35392 Giessen, Germany
[36] University of Chinese Academy of Sciences, Beijing 100049, People's Republic of China
[37] University of Hawaii, Honolulu, Hawaii 96822, USA
[38] University of Minnesota, Minneapolis, Minnesota 55455, USA
[39] University of Rochester, Rochester, New York 14627, USA
[40] University of Science and Technology of China, Hefei 230026, People's Republic of China
[41] University of South China, Hengyang 421001, People's Republic of China
[42] University of the Punjab, Lahore-54590, Pakistan
[43] (A)University of Turin, I-10125, Turin, Italy; (B)University of Eastern Piedmont, I-15121, Alessandria, Italy; (C)INFN, I-10125, Turin, Italy
[44] Wuhan University, Wuhan 430072, People's Republic of China
[45] Zhejiang University, Hangzhou 310027, People's Republic of China
[46] Zhengzhou University, Zhengzhou 450001, People's Republic of China

[a] Also at the Moscow Institute of Physics and Technology, Moscow 141700, Russia
[b] On leave from the Bogolyubov Institute for Theoretical Physics, Kiev 03680, Ukraine
[c] Also at the PNPI, Gatchina 188300, Russia
[d] Present address: Nagoya University, Nagoya 464-8601, Japan

Using a sample of 1.06×10^8 ψ' mesons collected with the BESIII detector at the BEPCII e^+e^- collider and χ_{cJ} mesons produced via radiative transitions from the ψ', we report the first observation for $\psi' \to \bar{p}K^+\Sigma^0 + c.c.$ (charge-conjugate), as well as improved measurements for the χ_{cJ} hyperon decays $\chi_{cJ} \to \bar{p}K^+\Lambda + c.c.$. The branching fractions are measured to be $\mathcal{B}(\psi' \to \bar{p}K^+\Sigma^0 + c.c) = (1.67\pm0.13\pm0.12)\times10^{-5}$, $\mathcal{B}(\chi_{c0} \to \bar{p}K^+\Lambda+c.c.) = (13.2\pm0.3\pm1.0)\times10^{-4}$, $\mathcal{B}(\chi_{c1} \to \bar{p}K^+\Lambda+c.c.) = (4.5 \pm 0.2 \pm 0.4) \times 10^{-4}$ and $\mathcal{B}(\chi_{c2} \to \bar{p}K^+\Lambda + c.c) = (8.4 \pm 0.3 \pm 0.6) \times 10^{-4}$, where the first error is statistical, and the second is systematic. In the decay of $\chi_{c0} \to \bar{p}K^+\Lambda + c.c.$, an anomalous enhancement near threshold is observed in the invariant mass distribution of $\bar{p}\Lambda + c.c.$, which cannot be explained by phase space.

PACS numbers: 13.25.Gv, 14.20.Jn, 14.40.Rt

I. INTRODUCTION

The study of hadronic decays of the $c\bar{c}$ states J/ψ, ψ', and χ_{cJ} could provide valuable information on perturbative QCD (pQCD) in the charmonium-mass regime and on the structure of charmonia. The color-octet mechanism (COM), which successfully described several decay patterns of the P-wave χ_{cJ} states [1], may be applicable to other χ_{cJ} decays. Measurements of χ_{cJ} hadronic decays may provide new input into COM and further assist in understanding the mechanisms of χ_{cJ} decays. Hadronic decays of charmonia below the $D\bar{D}$ mass threshold are also a good place to search for previously unknown meson states [2]. The BES Collaboration has previously reported observations of near-threshold structures in baryon-antibaryon invariant-mass distributions in the radiative decay $J/\psi \to \gamma p\bar{p}$ [3] and the purely hadronic decay $J/\psi \to p\bar{\Lambda}K^-$ [†] [4]. It has been suggested theoretically that these states may be observations of baryonium [5], or caused by final state interactions [6]. Studying the same decay modes in other charmonia may provide complementary information to improve the knowledge on these unexpected enhancements. It is also interesting to search for potential structures formed by $\Lambda\bar{\Lambda}$ and $p\bar{\Sigma}$ pairs, which could assist in extending the theoretical models.

BESIII has gathered a sample of 1.06×10^8 $e^+e^- \to \psi'$ events, which leads to abundant production of χ_{cJ} states

[†] Throughout the text, inclusion of charge conjugate modes is implied if not stated otherwise.

through radiative decays. This enables us to search for and study the hadronic decays of the χ_{cJ} states with high statistics.

II. DETECTOR

BEPCII [7] is a double-ring e^+e^- collider that has a peak luminosity reaching about 6×10^{32} $\mathrm{cm}^{-2}\mathrm{s}^{-1}$ at a center of mass energy of 3770 MeV. The BESIII [7] detector has a geometrical acceptance of 93% of 4π and has four main components: (1) A small-cell, helium-based (40% He, 60% C_3H_8) main drift chamber (MDC) with 43 layers providing an average single-hit resolution of 135 μm, and charged-particle momentum resolution in a 1 T magnetic field of 0.5% at 1 GeV/c. (2) An electromagnetic calorimeter (EMC) consisting of 6240 CsI(Tl) crystals in the cylindrical structure barrel and two endcaps. The energy resolution at 1.0 GeV is 2.5% (5%) in the barrel (endcaps), while the position resolution is 6 mm (9 mm) in the barrel (endcaps). (3) Particle Identification (PID) is provided by a time-of-flight system (TOF) constructed of 5-cm-thick plastic scintillators, with 176 detectors of 2.4 m length in two layers in the barrel and 96 fan-shaped detectors in the endcaps. The barrel (endcap) time resolution of 80 ps (110 ps) provides 2σ K/π separation for momenta up to $\sim$ 1.0 GeV/c. (4) The muon system (MUC) consists of 1000 m^2 of Resistive Plate Chambers (RPCs) in nine barrel and eight endcap layers and provides 2 cm position resolution.

III. MONTE-CARLO SIMULATION

Monte-Carlo (MC) simulation of the full detector is used to determine the detection efficiency of physics processes, optimize event selection criteria, and estimate backgrounds. The BESIII simulation program [8] provides an event generator, contains the detector geometry description, and simulates the detector response and signal digitization. Charmonium resonances, such as J/ψ and ψ', are generated by KKMC [9, 10], which accounts for the effects of initial-state radiation and beam energy spread. The subsequent charmonium meson decays are produced with BesEvtGen [11, 12]. The detector geometry and material description and the transportation of the decay particles through the detector including interactions are handled by Geant4 [13].

IV. DATA ANALYSIS

A. Event selection

Candidate $\psi' \to \bar{p}K^+\Sigma^0$ and $\psi' \to \gamma\chi_{cJ} \to \gamma\bar{p}K^+\Lambda$ events, with $\Sigma^0 \to \gamma\Lambda$ and $\Lambda \to p\pi^-$, are reconstructed using the following selection criteria.

Charged tracks must have their point of closest approach to the beamline within ± 30 cm of the interaction point in the beam direction ($|V_z| < 30$ cm) and within 15 cm of the beamline in the plane perpendicular to the beam ($V_r < 15$ cm), and must have the polar angle satisfying $|\cos\theta| < 0.93$. The time-of-flight and energy loss dE/dx measurements are combined to calculate PID probabilities for pion, kaon, and proton/antiproton hypotheses, and each track is assigned a particle type corresponding to the hypothesis with the highest confidence level (C.L.). For this analysis, four tracks identified as p, $\bar{p}$, K^+, and π^- are required. To suppress backgrounds from fake tracks, the $\bar{p}$ and K^+ are constrained to the same vertex by vertex fitting, and are required to satisfy $|V_z| < 10$ cm and $V_r < 1$ cm in the case of $\gamma\bar{p}K^+\Lambda$ modes, and the same procedure is applied for the respective antiparticle combinations in the charge-conjugate mode.

Photon candidates are selected in the EMC by requiring a minimum energy deposition of 25 MeV within the barrel region $|\cos\theta| < 0.8$, and 50 MeV within the endcap regions of $0.86 < |\cos\theta| < 0.92$. EMC cluster timing requirements suppress electronic noise and energy deposits unrelated to the event.

A kinematic fit that enforces momentum and energy conservation (4C) is applied with the hypothesis $\psi' \to \gamma p\bar{p}K^+\pi^-$, where the p and π^- are constrained by Λ decay vertex fitting. For the events with more than one photon candidate, the combination with the smallest χ^2_{4C} is retained for further analysis.

Λ candidates are selected by requiring the invariant mass of $p\pi^-$ to be within 7 MeV/c^2 of the mass of the Λ as given by the PDG [14], and this distribution is shown in Figure 1. Σ^0 candidates are formed by calculating the invariant mass of γ and Λ candidates, and this is shown in Figure 2(a).

After vetoing $\psi' \to \bar{p}K^+\Sigma^0$ events by removing events where the γ and Λ have an invariant mass within 15 MeV/c^2 of the Σ^0 mass [14], $\chi_{cJ}(J = 0, 1, 2)$ signals are seen distinctively in the spectrum of recoil mass against the γ, as shown in Figure 2(b).

B. Background studies

For the measurements of $\chi_{cJ} \to \bar{p}K^+\Lambda$, a sample of 1.06×10^8 inclusive ψ' MC events are used to investigate

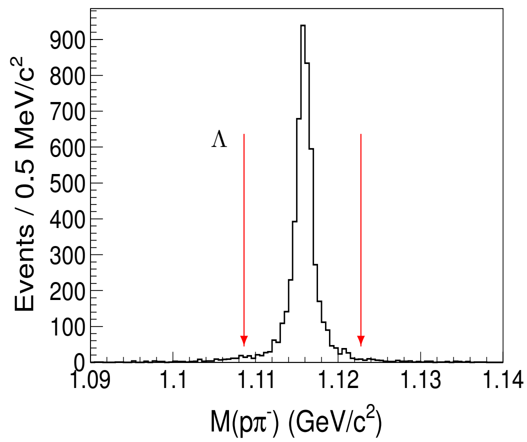

FIG. 1. (Color online) The invariant-mass distributions of $p\pi^-$. The vertical (red) arrows show the selection ranges around the Λ peak.

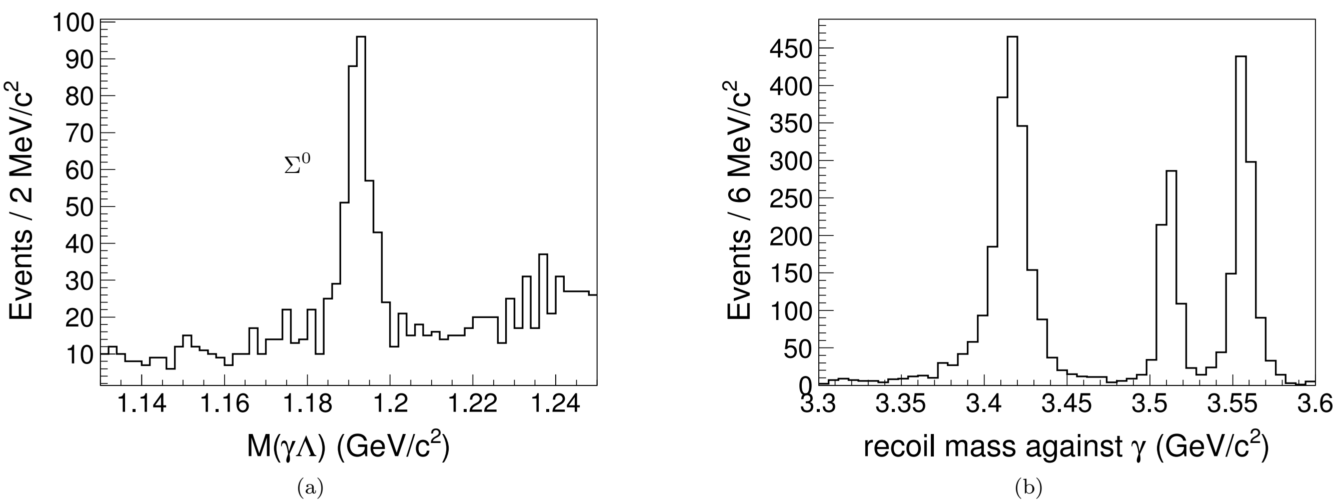

FIG. 2. Distributions of (a) the invariant masses of $\gamma\Lambda$ and (b) the recoil mass against the γ in decays of ψ' after vetoing $\psi' \to \bar{p}K^+\Sigma^0$ events.

possible backgrounds. The surviving events can be classified mainly into three decay processes: (1) $\psi' \to \bar{p}K^+\Lambda$, where a fake γ is produced; (2) $\psi' \to \pi^0\bar{p}K^+\Lambda$ where one γ from the π^0 decay escapes detection; and (3) the direct decay $\psi' \to \gamma\bar{p}K^+\Lambda$ having the same final topology with the signal, but not going through an intermediate χ_{cJ} state. Accordingly, 2×10^5 MC events for each of the three background processes are produced for further detailed studies. The same selection criteria are applied to the exclusive MC samples, and the surviving events are normalized to 1.06×10^8 total ψ' MC events. For the normalization procedure, the branching fraction $\mathcal{B} = (1.00 \pm 0.14) \times 10^{-4}$ for $\psi' \to \bar{p}K^+\Lambda$ is quoted in the PDG and the other two background modes have branching fractions in the order of 10^{-5}, which we roughly determine from our actual data sample. Figure 3(a) presents the distributions of the recoil mass against the γ for events that survive all cuts for the data and also for these background exclusive MC samples.

A similar study is also done for the measurement of $\psi' \to \bar{p}K^+\Sigma^0$ using the three background modes above together with $\psi' \to \gamma\chi_{cJ} \to \gamma\bar{p}K^+\Lambda \to \gamma p\bar{p}K^+\pi^-$, as shown in Figure 3(b).

In addition, a 42.9 pb^{-1} data sample, which is approximately a quarter of the luminosity at ψ' peak, collected at 3.65 GeV is used to investigate possible continuum backgrounds. Only 7 events survived inside the mass region of χ_{cJ} for the measurements of $\chi_{cJ} \to \bar{p}K^+\Lambda$, and are found to be negligible. For $\psi' \to \bar{p}K^+\Sigma^0$, 110 events from the continuum contribution must be subtracted after proper normalization according to the luminosities.

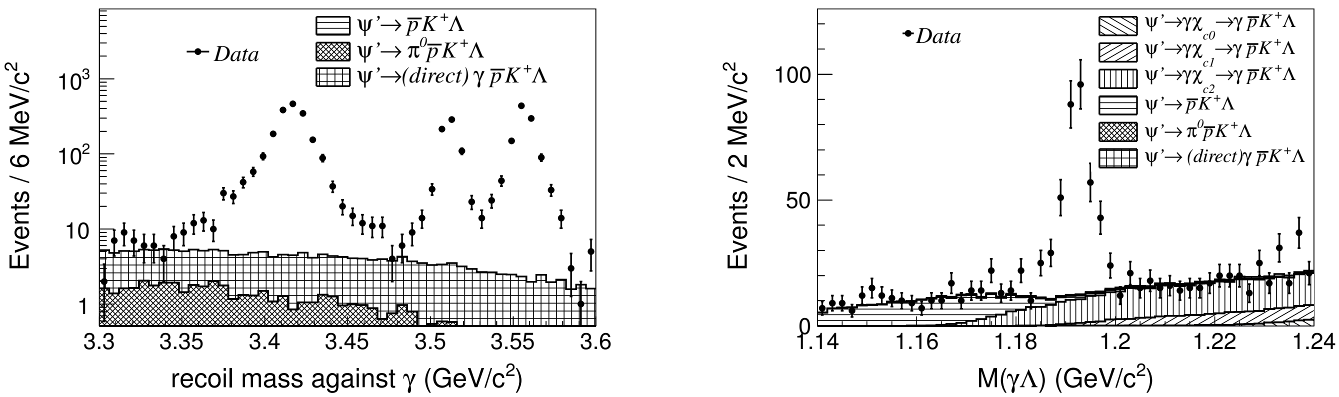

(a) (b)

FIG. 3. Comparison of data with exclusive MC samples for distributions of (a) the recoil mass against the γ for $\psi' \to \gamma\chi_{cJ} \to \gamma\bar{p}K^+\Lambda$ and (b) the $\gamma\Lambda$ invariant mass for $\psi' \to \bar{p}K^+\Sigma^0$. The MC samples have been normalized to the total number of ψ' events. In figure (a), the background from $\psi' \to \bar{p}K^+\Lambda$ events is too small to be visible.

C. Determination of branching fractions

1. Number of $\psi' \to \bar{p}K^+\Sigma^0$ events

The decay mode $\psi' \to \bar{p}K^+\Sigma^0$ is observed for the first time, with the main background processes $\psi' \to \gamma\bar{p}K^+\Lambda$, $\psi' \to \pi^0\bar{p}K^+\Lambda$, $\psi' \to \bar{p}K^+\Lambda$ and $\psi' \to \gamma\chi_{cJ} \to \gamma\bar{p}K^+\Lambda$. According to the studies in the previous section, the background shape can be described by a linear function, as shown in Figure 3(b).

A maximum likelihood fit is applied to the spectrum of the invariant mass of the selected γ and Λ, and we find a yield of 276 ± 21 events for the Σ^0 signal. The shape of the Σ^0 is obtained from MC simulation where the mass and width are fixed to the PDG values. The derived curves are shown in Figure 4, where dots with error bars represent the data with continuum contribution subtracted.

The detection efficiency for this process is determined to be 24.4% from MC simulation with a phase space model. The invariant mass spectra of $\bar{p}\Sigma^0$ and Σ^0K^+ are shown in Figure 5.

2. Number of $\psi' \to \gamma\chi_{cJ} \to \gamma\bar{p}K^+\Lambda$ events

For the $\chi_{cJ} \to \bar{p}K^+\Lambda$ decays, obvious inconsistencies exist in the distributions of $\bar{p}K^+$ and ΛK^+ invariant mass between the phase space MC and data, as shown in Figure 6, so the detection efficiencies for the decay modes $\psi' \to \gamma\chi_{c0,c1,c2} \to \gamma\bar{p}K^+\Lambda$ are determined by taking into account the dynamics of the decay.

For each χ_{cJ} state, the allowed regions of $M(\bar{p}K^+)$ versus $M(\Lambda K^+)$ are divided into 25×25 areas of equal length (40 MeV/c^2 for χ_{c0} and 48 MeV/c^2 for χ_{c1} and χ_{c2}), and each area is tagged with an index ij. For each area the number of events $N^{ij}_{\rm data}$ for data and detection efficiency ϵ_{ij} are determined individually. Then, the total number of events ($N_{\rm cor}$) is calculated as $N_{\rm cor} = \Sigma_{ij}\frac{N^{ij}_{\rm data}}{\epsilon_{ij}}$. Samples of 5.5×10^6 MC events are used to determine the detection efficiencies ϵ_{ij} of each area for $\chi_{c0}, \chi_{c1}, \chi_{c2}$, respectively.

The data belonging to χ_{c0}, χ_{c1}, and χ_{c2} are separated using mass windows on the distribution of recoil mass against the detected γ of 3.35–3.48, 3.49–3.53, and 3.53–3.59 GeV/c^2, respectively. When extracting $N^{ij}_{\rm data}$, the background has been subtracted using exclusive MC samples according to the results of background studies. The calculated total numbers of events $N_{\rm cor}$ are listed in Table I.

TABLE I. The total numbers of events $N_{\rm cor}$ for each $\chi_{cJ} \to \bar{p}K^+\Lambda$ are derived from $N_{\rm cor} = \Sigma_{ij}\frac{N^{ij}_{\rm data}}{\epsilon_{ij}}$. $N_{\rm error}$ is the propagated error.

Modes	$N_{\rm cor}$	$N_{\rm error}$
χ_{c0}	8642.7	201.3
χ_{c1}	2824.0	112.6
χ_{c2}	4961.0	154.4

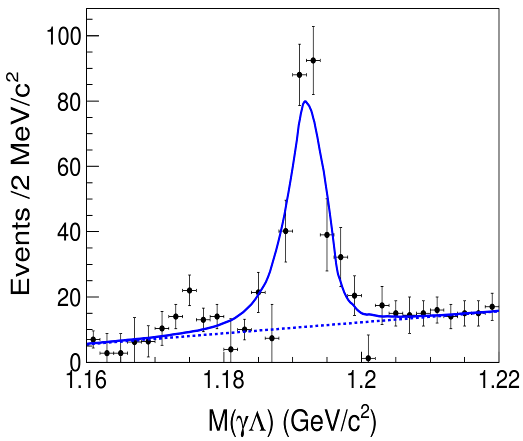

FIG. 4. (Color online) The shape of the Σ^0 signal as derived from MC simulations which had the mass and width fixed to the PDG values. The fit result is shown by the solid line with a linear background indicated by the dashed line. The data points with error bars show the data, where the continuum contribution has already been subtracted.

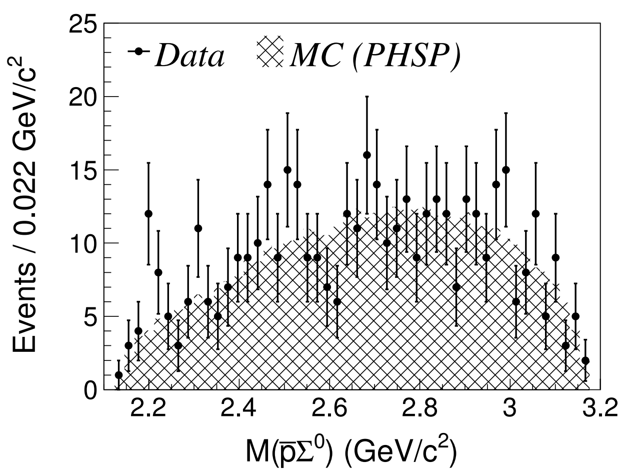

(a)

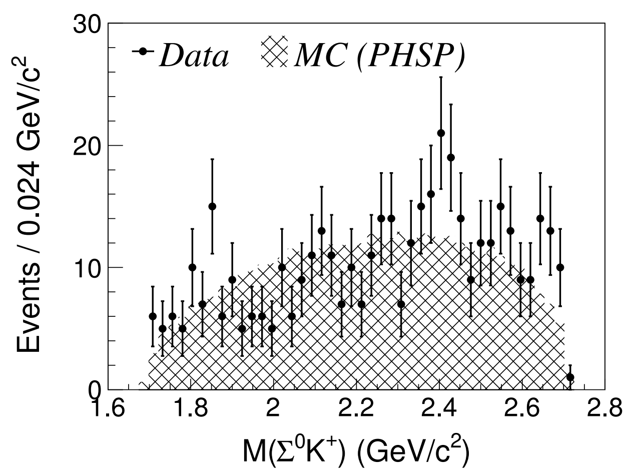

(b)

FIG. 5. Invariant mass spectra of (a) $\bar{p}\Sigma^0$ and (b) $\Sigma^0 K^+$ for the reaction $\psi' \to \bar{p}K^+\Sigma^0$. Dots are the data and the hatched regions describe MC events generated according to a phase space model.

3. *Calculation of branching fractions*

The branching fraction of $\psi' \to \bar{p}K^+\Sigma^0$ is calculated with

$$\mathcal{B} = \frac{N_{\rm obs}}{N_{\psi'} \cdot \mathcal{B}_{\Sigma^0\to\gamma\Lambda} \cdot \mathcal{B}_{\Lambda\to p\pi} \cdot \epsilon},$$

where $N_{\psi'}$ is the total number of ψ' events, which is measured to be 1.06×10^8 with an uncertainty of 0.81% [15]; the branching fractions (63.9±0.5)% for $\mathcal{B}_{\Lambda\to p\pi}$ and 100% for $\mathcal{B}_{\Sigma^0\to\gamma\Lambda}$ are taken from the PDG [14]; $N_{\rm obs}$ means the observed number of signals derived from the fit and ϵ is the detection efficiency from MC simulation.

The branching fractions for each $\chi_{c0,c1,c2} \to \bar{p}K^+\Lambda$ are calculated similarly with

$$\mathcal{B} = \frac{N_{\rm cor}}{N_{\psi'} \cdot \mathcal{B}_{\psi'\to\gamma\chi_{cJ}} \cdot \mathcal{B}_{\Lambda\to p\pi}},$$

where the branching fractions of the χ_{cJ} states ((9.68 ± 0.31)%, (9.2±0.4)% and (8.72±0.34)% for $\mathcal{B}(\psi' \to \gamma\chi_{c0})$, $\mathcal{B}(\psi' \to \gamma\chi_{c1})$ and $\mathcal{B}(\psi' \to \gamma\chi_{c2})$, respectively) are taken from the PDG [14].

D. Near-threshold structure

The large discrepancies between the data and phase space MC samples in Figure 6 imply that intermediate

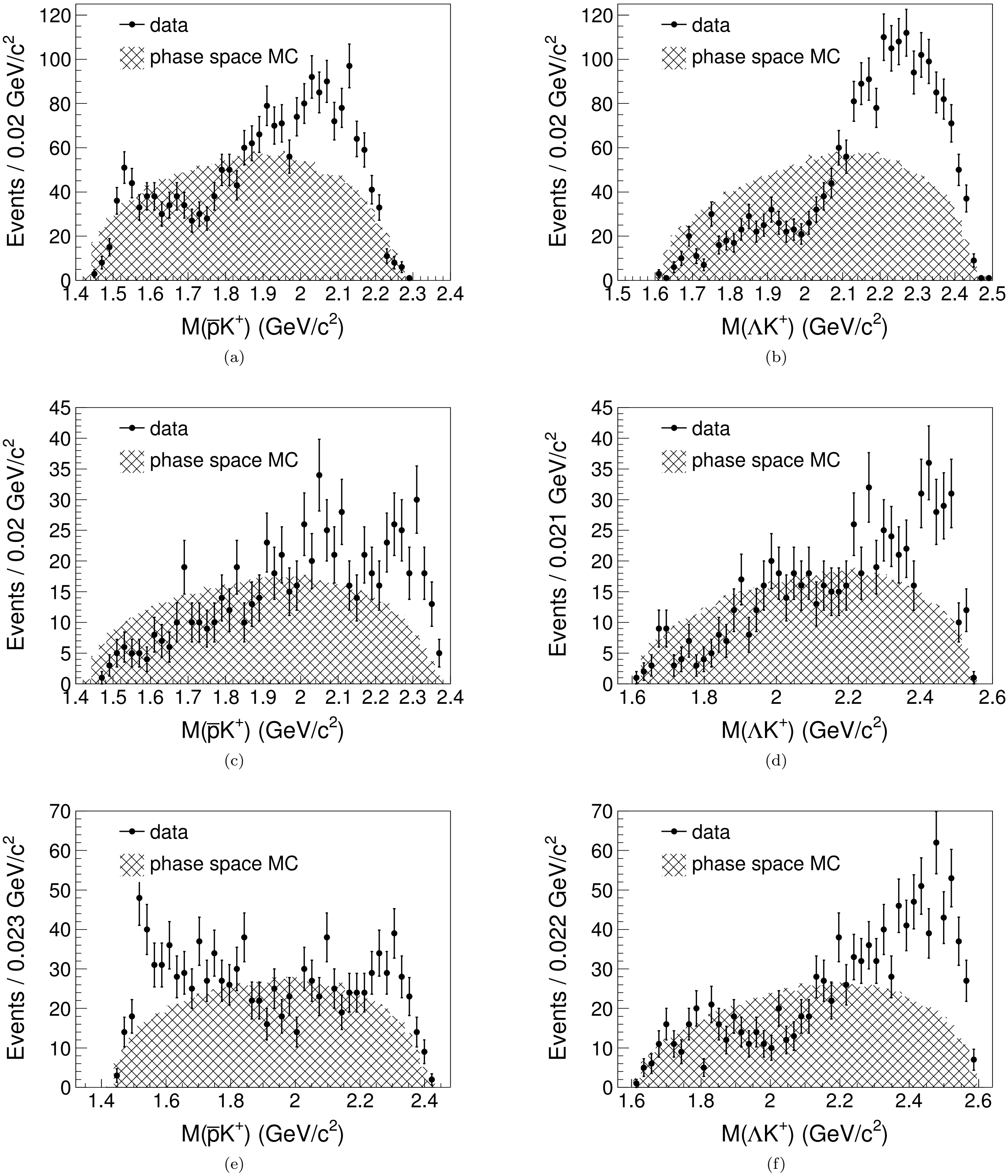

FIG. 6. Invariant mass spectra of $\bar{p}K^+$ and ΛK^+ for (a, b) χ_{c0}, (c, d) χ_{c1} and (e, f) χ_{c2}. The dots are the data, and the hatched regions show the distribution of MC events generated according to a phase space model. Potential intermediate states, such as the $\bar{\Lambda}(1520)$ and $N(1710)$, are seen in the invariant mass distributions of $\bar{p}K^+$ and ΛK^+, respectively.

states exist in the decays of $\chi_{cJ} \to \bar{p}K^+\Lambda$. Possible structures are observed in the Dalitz plots shown in Figure 7, and particularly for the χ_{c0}, it seems that there is a structure in the near-threshold region of $M(\bar{p}\Lambda)$ reflected by the anomalous enhancement in the top right corner of the Dalitz plot.

Figure 8(a) shows the invariant-mass distribution of $\bar{p}\Lambda$ for $\chi_{c0} \to \bar{p}K^+\Lambda$, where the dashed line denotes the phase space distribution that has been normalized to the signal yield and the dots present efficiencies in each bin. Evident discrepancies are seen near the threshold region. Due to insufficient statistics, in this analysis a simple fit with a Breit-Wigner function to this region is done without considering quantum mechanical interference. The fit curve for the near-threshold structure is depicted in Figure 8(b), where the distribution of $M(\bar{p}\Lambda)$ has been corrected by the detector efficiency. The structure can be fit well with a weighted Breit-Wigner function of the form

$$f(M) \propto \frac{q^{2L+1}k^{L'+1}}{(M^2 - M_0^2)^2 - M_0^2\Gamma^2} \qquad (1)$$

where q is the anti-proton momentum in the $\bar{p}\Lambda$ rest frame, k is the kaon momentum in the χ_{c0} rest frame, L (L') denotes the orbital angular momentum between the antiproton and Λ (between the kaon and $\bar{p}\Lambda$). On the basis of conservation on J^P, in the decays of χ_{c0}, "$L + L'$ = even number" can be inferred, and therefore the only possible spin-parity combinations are $J^P = 0^-$, 1^+, 2^-, $\cdots$. Because the structure is near the $\bar{p}\Lambda$ threshold, the relative orbital angular momentum between the antiproton and Λ is most likely 0. Therefore, $J^P = 0^-$ is used in the fitting process which gives $M = 2.053 \pm 0.013$ GeV $/c^2$ and $\Gamma = 292 \pm 14$ MeV for the Breit-Wigner mass and width parameters. A shape of the phase space MC is added to describe the background in the fitting, which is shown as the dashed line in Figure 8(b).

For $\psi' \to \bar{p}K^+\Sigma^0$, the invariant-mass spectrum of $M(\bar{p}\Sigma^0)$ was shown in Figure 5(a). In this channel, there may be similar structures close to the $\bar{p}\Sigma^0$ threshold, but there is a large uncertainty due to the relatively small sample size.

V. SYSTEMATIC UNCERTAINTIES

The main contributions to the systematic uncertainties in the measurements of the branching fractions originate primarily from the tracking, PID, photon reconstruction, kinematic fit, branching fractions of intermediate states, total number of ψ' events, and the fitting procedure. The results are summarized in Table II.

The tracking efficiency for MC simulated events is found to agree with the data within 1% for each charged track coming from a primary vertex from analyses of $J/\psi \to K^*K$ and $J/\psi \to p\bar{p}\pi^+\pi^-$ events. For each track from Λ (or $\bar{\Lambda}$), the uncertainty is also 1% according to a study of very clean $J/\psi \to \bar{p}K^+\Lambda$ events.

The candidates for the selected final states require tracks to be identified as p, $\bar{p}$, K^+ or π^-. Comparing data and MC event samples for $J/\psi \to \bar{p}K^+\Lambda$ and $J/\psi \to K^*K$, the difference between MC and data for the particle identification efficiency was found to be 2% for the antiproton, 1% for the proton and kaon, and negligible for charged pions.

The difference in the reconstruction efficiency between the data and MC is about 1% per photon [16].

To estimate the uncertainty from kinematic fitting, the kinematic fitting efficiency is studied using events of $\psi' \to \gamma\chi_{c0} \to \gamma p\bar{p}\pi^+\pi^-$ and the difference between data and MC is found to be 2.8%.

Uncertainties due to the mass window requirement for the Λ signal are studied with the control sample $\psi' \to \bar{p}K^+\Lambda$. The efficiency difference between data and MC is obtained to be 0.4%.

Uncertainties in the fitting procedure are obtained by varying fit intervals and changing the linear background shape to a 2$^{\text{nd}}$ order Chebyshev polynomial or a MC background shape. It contributes a 3.3% uncertainty to the measurement of $\psi' \to \bar{p}K^+\Sigma^0$.

The uncertainty on the total number of ψ' events was found to be 0.81% by studying inclusive hadronic ψ' decays [15].

Uncertainties due to the branching fractions of $\psi' \to \gamma\chi_{cJ}$ are 3.2%, 4.3% and 3.9% for each χ_{c0}, χ_{c1} and χ_{c2}, respectively [14]. The uncertainty due to the branching fraction of $\Lambda \to p\pi^-$ is 0.8% [14].

Uncertainties due to the numbers of areas in the procedure of calculating total numbers of events for $\psi' \to \gamma\chi_{cJ} \to \gamma\bar{p}K^+\Lambda$ are shown as "2D Binning" in Table II. Detection efficiencies are assumed to be constant within each of these 25×25 sub-areas (see section IV C 2), and as a check, we varied the number of areas. Besides the original 25×25 binning, three other divisions (20×20, 30×30, 35×35) were tried, and the largest differences among them are taken into account as the systematic uncertainty due to the binning.

Uncertainties from the mass window requirements of χ_{c0}, χ_{c1} and χ_{c2}, obtained by changing the χ_{cJ} selection window, are shown as item "Mass Window" in Table II, and are small compared to other errors.

A possible Λ polarization in the decays of χ_{cJ} might affect detection efficiencies and yield different results. With our limited statistics, it was not possible to measure the polarization of the Λ in fine bins of the Dalitz plot for each χ_{cJ} state, but an overall measurement of the Λ polarization P was done for each χ_{cJ} state that yielded $P = 0.04 \pm 0.07$ for χ_{c0}, -0.17 ± 0.12 for χ_{c1}, and 0.22 ± 0.09 for χ_{c2}. Subsequently, new samples of MC events were then generated with the Λ having this

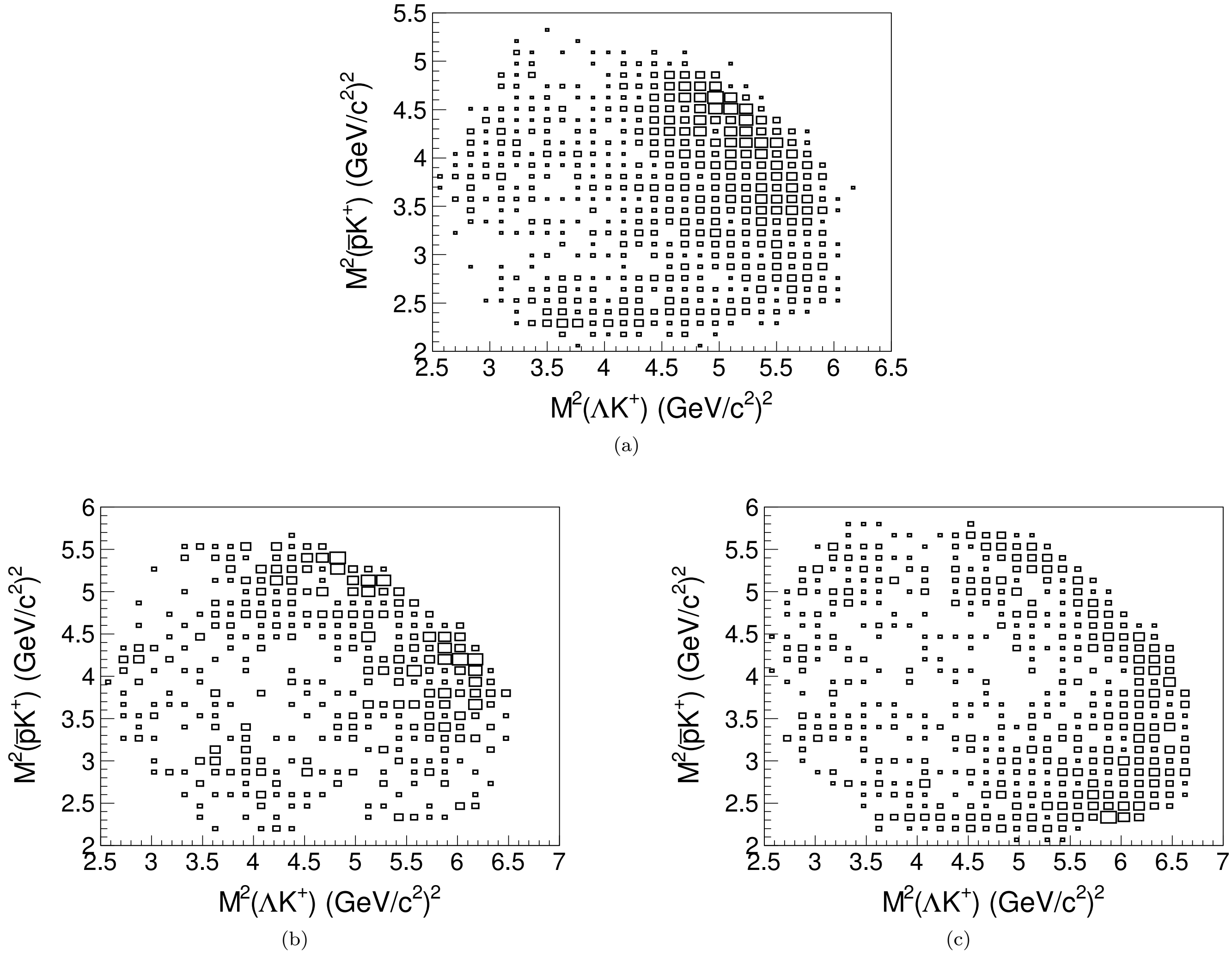

FIG. 7. Dalitz plots of $M^2(\bar{p}K^+)$ versus $M^2(\Lambda K^+)$ for (a) χ_{c0}, (b) χ_{c1} and (c) χ_{c2}. A concentration of events in the upper right corner shows an enhancement at the $\bar{p}\Lambda$ threshold.

polarization P, so that the decay distributions are given by $1 + \alpha P \cos\Theta$, where Θ is the angle between the Λ flight direction in the χ_{cJ} rest frame and the π direction in the Λ rest frame, and α is the weak decay parameter for the Λ. The difference in efficiencies with respect to that of phase space MC samples are taken as a systematic uncertainty.

The total systematic uncertainty is obtained by summing up uncertainties contributed from all individual sources in quadrature.

VI. RESULTS AND DISCUSSION

We observe the decay mode $\psi' \to \bar{p}K^+\Sigma^0 + c.c.$ for the first time and improve the measurements for the decays of $\chi_{cJ} \to \bar{p}K^+\Lambda + c.c.$, using 1.06×10^8 ψ' events collected with BESIII detector at the BEPCII collider. The branching fractions are listed in Table III.

For the $\bar{p}K^+\Lambda + c.c.$ final state in the decays of χ_{c0}, an anomalous enhancement is observed in the invariant-mass distribution of $\bar{p}\Lambda + c.c.$, which could correspond to the structure observed in the decay $J/\psi \to p\bar{\Lambda}K^-$ [4]. It is of great interest that the structure is located very close to the mass threshold of $\bar{p}\Lambda + c.c.$, and this may be accounted for as a quasibound dibaryon state or as an enhancement due to a final-state interaction, or simply as an interference effect of high-mass N^* and Λ^*. Our new measurements may aid in the theory of charmonia decays, and also be a guide in the calculation of decay modes into strangeness dibaryon systems. A detail study on the near-threshold structure is expected with larger statistics in future BESIII running.

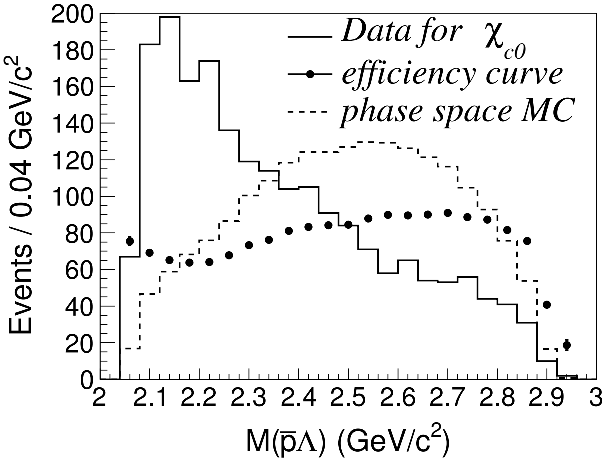

(a)

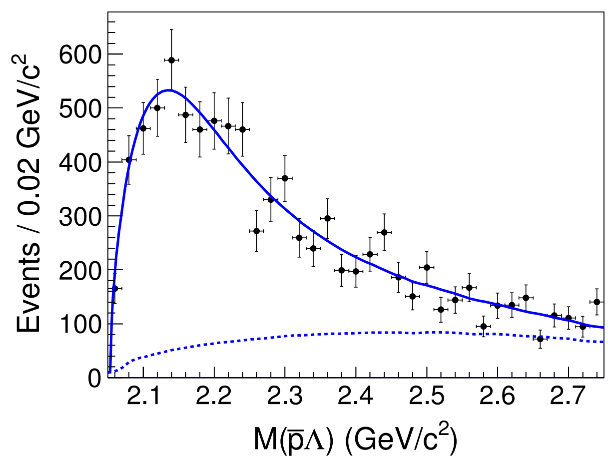

(b)

FIG. 8. (Color online) (a) Invariant-mass distribution of $\bar{p}\Lambda$ for $\chi_{c0} \to \bar{p}K^+\Lambda$, where the dashed line denotes the phase space distribution that has been normalized to the signal yield. The histogram shows the data and dots present the efficiency curve. (b) Fit result to a Breit-Wigner function with $J^P = 0^-$ after acceptance correction. The dashed line describes the background shape from phase space MC events.

TABLE II. Systematic uncertainties in the measurements of the branching fractions in percent (%)

	$\psi' \to \bar{p}K^+\Sigma^0$	$\chi_{cJ} \to \bar{p}K^+\Lambda$		
		χ_{c0}	χ_{c1}	χ_{c2}
Tracking	4.0	4.0	4.0	4.0
PID	4.0	4.0	4.0	4.0
Photon Recon.	1.0	1.0	1.0	1.0
Kinematic Fit	2.8	2.8	2.8	2.8
Fitting	3.3	− − −	− − −	− − −
Λ mass window	0.4	0.4	0.4	0.4
Intermediate states	0.8	3.3	4.4	4.0
$N_{\psi'}$	0.81	0.81	0.81	0.81
2D Binning	− − −	1.3	0.7	1.1
Mass Window	− − −	< 0.1	0.7	0.4
Λ Polarization	− − −	1.3	0.4	1.8
Total	7.3	7.5	7.9	7.6

ACKNOWLEDGMENTS

The BESIII collaboration thanks the staff of BEPCII and the computing center for their hard efforts. This work is supported in part by the Ministry of Science and Technology of China under Contract No. 2009CB825200; National Natural Science Foundation of China (NSFC) under Contracts Nos. 10625524, 10821063, 10825524, 10835001, 10935007, 11005109, 11079030, 11125525, 11179007, 11275189; Joint Funds of the National Natural Science Foundation of China under Contracts Nos. 11079008, 11179007; the Chinese Academy of Sciences (CAS) Large-Scale Scientific Facility Program; CAS under Contracts Nos. KJCX2-YW-N29, KJCX2-YW-N45; 100 Talents Program of CAS; Research Fund for the Doctoral Program of Higher Education of China under Contract No. 20093402120022; German Research Foundation DFG under Contract No. Collaborative Research Center CRC-1044; Istituto Nazionale di Fisica Nucleare, Italy; Ministry of Development of Turkey under Contract No. DPT2006K-120470; U. S. Department of Energy under Contracts Nos. DE-FG02-04ER41291, DE-FG02-94ER40823; U.S. National Science Foundation; University of Groningen (RuG) and the Helmholtzzentrum fuer Schwerionenforschung GmbH (GSI), Darmstadt; WCU Program of National Research Foundation of Korea under Contract No. R32-2008-000-10155-0

TABLE III. The branching fractions for $\psi' \to \bar{p}K^+\Sigma^0 + c.c.$ and $\chi_{cJ} \to \bar{p}K^+\Lambda + c.c.$, where the first errors are statistical and second ones systematic.

channel	$\psi' \to \bar{p}K^+\Sigma^0 + c.c.$	$\chi_{c0} \to \bar{p}K^+\Lambda + c.c.$	$\chi_{c1} \to \bar{p}K^+\Lambda + c.c.$	$\chi_{c2} \to \bar{p}K^+\Lambda + c.c.$
$\mathcal{B}$(BESIII)	$(1.67 \pm 0.13 \pm 0.12) \times 10^{-5}$	$(13.2 \pm 0.3 \pm 1.0) \times 10^{-4}$	$(4.5 \pm 0.2 \pm 0.4) \times 10^{-4}$	$(8.4 \pm 0.3 \pm 0.6) \times 10^{-4}$
PDG		$(10.2 \pm 1.9) \times 10^{-4}$	$(3.2 \pm 1.0) \times 10^{-4}$	$(9.1 \pm 1.8) \times 10^{-4}$

[1] S. M. Wong, Eur. Phys. J. C **14**, 643 (2000).

[2] E. Klempt, A. Zaitsev, Physics Reports **454**, 1-202, (2007).

[3] J. Z. Bai *et al.* (BES Collaboration), Phys. Rev. Lett. **91**, 022001 (2003).

[4] M. Ablikim *et al.* (BES Collaboration), Phys. Rev. Lett. **93**, 112002 (2004).

[5] A. Datta, P. J. O'Donnell, Phys. Lett. B **567**, 273 (2003).
B. Loiseau, S. Wycech, Phys. Rev. C **72**, 011001(R) (2005).
M.-L. Yan, S. Li, B. Wu, B.-Q. Ma, Phys. Rev. D **72**, 034027 (2005).

[6] B. Kerbikov, A. Stavinsky, and V. Fedotov, Phys. Rev. C **69**, 055205 (2004).
J. Haidenbauer, U.-G. Meissner, A. Sibirtsev, Phys. Rev. D **74**, 017501 (2006).
D. R. Entem, F. Fernandez, Phys. Rev. D **75**, 014004 (2007).

[7] M. Ablikim *et al.* (BESIII Collaboration), Nucl. Instrum. Meth. A **614**, 345 (2010)

[8] Z. Y. Deng *et al.*, Chin. Phys. C **30**, 371 (2006)

[9] S. Jadach, B.F.L. Ward and Z. Was, Comp. Phys. Commu. **130**, 260 (2000)

[10] S. Jadach, B.F.L. Ward and Z. Was, Phys. Rev. **D63**, 113009 (2001)

[11] D. M. Asner *et al.*, Modern Physics A, **24** No.1 (supp.) (2009)

[12] R. G. Ping, Chin. Phys. C **32**, 599 (2008)

[13] S. Agostinelli *et al.* (GEANT Collaboration), Nucl. Instrum. Meth. A **506**, 250 (2003); J. Allison *et al.*, IEEE Trans. Nucl. Sci. **53**, 270 (2006).

[14] J. Beringer *et al.* (Particle Data Group), Phys. Rev. **D86**, 010001 (2012)

[15] M. Ablikim *et al.* (BESIII Collaboration), arXiv:1209.6199, to be published in Chinese Physics C

[16] M. Ablikim *et al.* (BESIII Collaboration), Phys. Rev. D **83**, 112005 (2011)